Quantitative molecular interpretation of mesoscopic correlations in bicontinuous microemulsions

Hyung-June Woo, Carlo Carraro, and David Chandler
Department of Chemistry, University of California, Berkeley, California 94720-1460
(Received 30 June 1995)

The charge frustrated Ising model is used as the basis for understanding bicontinuous oil-water-surfactant mixtures. The elemental energy of the model is related to the surface tension between oil and water in the absence of surfactant. The two elemental lengths of the model are related to the volume of a water molecule (or oil segment) and the length of a surfactant molecule. The model is analyzed analytically with approximations justified for homogeneous mixtures on length scales that are larger than these microscopic lengths. The symmetry and discreteness of the underlying lattice are physically irrelevant in this regime. The local mean field approximation is applied to the model yielding a theory that is consistent with the Landau-Ginzburg phenomenology of microemulsions. Corrections to the mean field treatment are required for a quantitative description of the correlations of bicontinuous microemulsions. In analyzing these corrections, a theory is derived that is related to the random wave model, but with all phenomenological coefficients now determined in terms of temperature, surfactant density, and surfactant chain length. A comparison with existing experimental data is successful. Predictions and suggestions are made for future experiments.

PACS number(s): 82.70.Kj, 05.50.+q, 61.20.Gy, 61.25.Em

I. INTRODUCTION

The phenomenon of microphase separation is common to many physical systems such as diblock copolymers and amphiphilic mixtures. By far the best studied and best understood systems displaying microphase separation are oil-water-surfactant ternary mixtures. The large body of available experimental data [1] and the very rich and interesting phenomenologies have stimulated a strong theoretical effort in the past decade [2]. While most of the observed phenomena are now well understood qualitatively, quantitative comparison of experiments with microscopic (first principles) theory has been rare. The present work is oriented in that direction. In particular, it is now understood that frustration, arising from competing interactions over different length scales, plays a crucial role in microphase separation [2–4]. Our goal is to identify both range and strength of these interactions in terms of experimentally accessible parameters, such as molecular lengths, densities, and temperature.

Consider first a binary mixture of a polar species P and a hydrophobic species H (e.g., water and oil). Below the critical point, the mixture phase separates into two phases, one rich in H and the other rich in P. Within each phase, the only fluctuations that occur have a small correlation length, a. The length is microscopic, typically less than 5 Å in size.

Consider next what happens when a small amount of surfactant is added to the binary mixture. Surfactants are long amphiphilic molecules that are P-like at one end, and H-like at the other end. We use P_S and H_S, respectively, to denote the polar and hydrophobic segments of the surfactant molecules. These molecules preferentially exist at the P-H interface, so that heads and tails can reside in the preferred component. If the concentration of surfactant is large enough that the interface is saturated, accommodating additional surfactant within a single phase, say P, will force an excess of species H_S into the "wrong" phase. If the length of the surfactant molecules, Δ, exceeds the correlation length of the spontaneous fluctuations of the binary mixture, $\Delta \gg a$, the presence of surfactants within the bulk phases frustrates the system. In this case, surfactant molecules self-assemble to minimize the exposure of the P_S and H_S ends to the H and P phases, respectively. The result is the formation of self-assembled structures, such as micelles and bilayers, or the formation of large coexisting domains or interconnected channels of P and H. In the latter case, the system is homogeneous and disordered over macroscopic length scales, but is highly inhomogeneous over mesoscopic length scales (as large as several hundred angstroms). It is microphase separated.

Many of these structures involve correlation lengths that are very large compared to either a or Δ. As such, a theory for them should require only a few microscopic parameters pertaining to the molecules that comprise the material. This concept is familiar in the theory of simple fluids where a single energy and one microscopic length prove satisfactory. The principle of corresponding states follows from this minimalist description. For a simple fluid, the energy parameter determines the critical temperature, or equivalently, the surface tension between coexisting phases far from the critical point. The microscopic length is essentially the diameter of a molecule, or equivalently, the correlation length far from the critical point. One theme of this current paper is that only one additional length is required to capture much of the mesoscopic behavior of complex fluids. The second length is Δ, the typical distance between H_S and P_S groups within a surfactant molecule.

The length Δ is associated with the constraint of stoichiometry. This constraint affects the entropy of the system. Stillinger [5] and others [6] have noted that this entropy contribution can be estimated from an electrostatic analogy. Accessible fluctuations of P_S and H_S densities are those that maintain stoichiometry with intramolecular length Δ. Similarly, accessible charge particle fluctuations are those that maintain electroneutrality on the scale of the Debye screening length, r_D. Generally, field-theoretic implications of a length scale constraint can be mapped to an interaction that is Coulombic in form [7]. For the specific case of surfactants with mean bulk density ρ, the strength of the Coulombic interaction is governed by the charge, q, given by [5]

$$q^2 = d/4\pi\beta\rho\Delta^2. \tag{1.1}$$

In this equation, d denotes dimensionality, and $\beta^{-1} = k_BT$. The Debye length associated with this charge is indeed $\sim \Delta$.

Exploiting this electrostatic analogy, Stillinger constructed a density field theory for surfactant-water mixture [5]. His numerical work established that the model predicts the formation of micelles and lamellae. Leibler, and also Ohta and Kawasaki [6] have studied similar models in the context of diblock copolymer melts. Hurley and Singer have illustrated how frustration by long-ranged interactions, Coulombic in origin, leads to spatially modulated phases of two-dimensional films [8]. Deem and Chandler [9,10] carried out an analysis of bicontinuous phases based upon a slight generalization of Stillinger's continuum model. With physically reasonable values of parameters, Deem and Chandler were able to fit experimental structure factor data successfully. However, to account for the nonlinearity of the system, a rather complicated numerical scheme was needed in their approach, obscuring the underlying physical picture.

We can simplify Deem and Chandler's analysis considerably by working with a corresponding lattice model. This charge frustrated Ising model was introduced by Wu, Chandler, and Smit [11]. It is discussed in the next section where an approximate reduced version of the model is also derived. The reduction is appropriate for the description of bicontinuous microemulsion phases. While the reduced version bears some resemblance to Widom's lattice model [3], the approach we take is distinct. The results we derive from the reduced model are free of artifacts due to the underlying lattice, and we are able to successfully relate experimental observations to molecular parameters, such as Δ.

An analytical treatment of the reduced model is carried out within mean-field theory in Sec. III. A more accurate analysis is needed to treat experimental results in a meaningful quantitative fashion. Such an analysis that accounts for fluctuations is given in Sec. IV. The development here is similar to the random wave model [16–19], but with phenomenological coefficients now determined in terms of microscopic quantities. Comparison with small-angle neutron scattering (SANS) experiments [1,12–15] is made in Sec. V. We conclude in Sec. VI with a brief discussion. An Appendix is used to discuss some details of the analysis omitted from Sec. II.

II. THE LATTICE MODEL

A. Hamiltonian

We consider a cubic lattice with spacing a, and two binary variables: $s_i = \pm 1$, indicating whether lattice site i is occupied by a polar or hydrophobic species, and $t_i = 1, 0$, indicating whether that species is or is not part of a surfactant (if it is not, the species corresponds to water or oil). The charge frustrated Hamiltonian for these variables is

$$\mathcal{H}[s_i, t_i] = \mathcal{H}_S[s_i] + \mathcal{H}_C[s_i, t_i] \ , \tag{2.1a}$$

$$\mathcal{H}_S = -\frac{1}{2}\sum_{ij} J_{ij} s_i s_j - \sum_i h_i s_i \ , \tag{2.1b}$$

$$\mathcal{H}_C = \frac{q^2}{2}\sum_{i\neq j} v_{ij} s_i s_j t_i t_j - \mu \sum_i t_i. \tag{2.1c}$$

The quantity μ is the chemical potential that controls the relative amount of surfactants. The corresponding quantities controlling the concentrations of oil and water are absorbed into the spatially dependent field h_i. The nearest-neighbor ferromagnetic interaction

$$J_{ij} = \begin{cases} J & > 0, \ r_{ij} = a, \\ 0, & \text{otherwise}, \end{cases}$$

expresses the preference of oil and water to phase separate (r_{ij} denotes the distance between cells i and j). The sites with frustrating charges interact via the nearest neighbor interactions plus the Coulomb potential governed by

$$\begin{aligned} v(r_{ij}) &= \frac{1}{N}\sum_{\mathbf{k}} \frac{4\pi}{a^3k^2} \exp(i\mathbf{k}\cdot\mathbf{r}_{ij}) \\ &\simeq \int_{\mathbf{k}} \frac{4\pi}{a^3k^2} \exp(i\mathbf{k}\cdot\mathbf{r}_{ij}), \end{aligned} \tag{2.2}$$

where N is the total number of sites and

$$\int_{\mathbf{k}} \equiv \left(\frac{a}{2\pi}\right)^3 \int_{|\mathbf{k}|\leq k_c} d\mathbf{k}. \tag{2.3}$$

The quantity $k_c \sim a^{-1}$ is the microscopic wave-vector cutoff. (We work in three dimensions. Extensions to other dimensions is straightforward.) The condition of normalization,

$$\frac{1}{N}\sum_{\mathbf{k}} 1 = 1 \tag{2.4}$$

gives

$$k_c \simeq (6\pi^2/a^3)^{1/3}. \tag{2.5}$$

The approximation converting the sum over wave vectors in the first Brillouin zone to an integral in spherical coordinates is justified for length scales fairly large compared

to the microscopic lattice spacing a (i.e., $ka \ll 1$). This is the regime we are concerned with. Indeed, the concept of charge frustration is valid only for $k \lesssim 1/\Delta$. The results of our analysis will be independent of the specific details of the underlying lattice structure for the corresponding length scales.

The basic parameters of the model are a, J, and Δ. The lattice spacing a corresponds to the correlation length of water or alkane chains. Roughly, we can think of each lattice site as being occupied by a water molecule or one unit of the oil or surfactant alkane chain. For temperatures well below the critical demixing temperature of oil-water mixtures, the short-range interaction energy scale J can be related to σ, the oil-water surface tension in the absence of surfactant:

$$J = \sigma a^2/2. \tag{2.6}$$

At room temperature, a typical value of surface tension is $\sigma \simeq 50$ erg/cm^2 $\simeq 0.1 k_B T$ Å^{-2} [20]. The lattice gas model that is consistent with this value of surface tension and the compressibility (or mean-square density fluctuations) of water has $a \simeq 2$ Å. The other length scale, Δ, is the root-mean-square separation between head and tail groups in a surfactant molecule [21]. The typical magnitude of Δ will be from $\Delta \sim 5$ Å for short-chain surfactants, to tens of angstroms for long-chain surfactants, and even longer for diblock copolymers.

In this lattice Hamiltonian, for each surfactant molecule, there is a corresponding pair of charged sites. The density of polar surfactant segments at lattice site i is

$$\rho_{P_S}(i) = (1 + s_i) n_{P_S} t_i / 2a^3, \tag{2.7}$$

where n_{P_S} is the number of polar segments per surfactant. Similarly, the hydrophobic surfactant segment density, $\rho_{H_S}(i)$, is $(1 - s_i) n_{H_S} t_i / 2a^3$. Within a surfactant, n_α sites (α either P_S or H_S) are constrained to move together. As such, they are replaced by one charged site in the lattice model. Flory's entropy factor for the mixing of polymers follows from the same observation [22]. The spins, s_i, do not represent molecules or segment of molecules, *per se*, but rather, they provide a discrete representation of density fields.

The lattice cells have a volume much smaller than that occupied by a surfactant molecule composed of several segments. Therefore, the connectivity of a surfactant is not fully accounted for. This feature would generally underestimate the effect of surfactants frustrating the phase separation, especially for long-chain surfactants. The error can be alleviated by regarding

$$f = 2\rho a^2 \Delta \tag{2.8}$$

as the volume fraction of surfactants. This formula is motivated by the fact that the length and cross-sectional area of a surfactant molecule are roughly 2Δ and a^2, respectively.

The preceding discussion emphasizes that all parameters in the model have clear physical meaning directly related to experimental conditions with known typical values. This recognition is the first step in making quantitative comparison with experiments possible.

B. Reduction of the model

The partition function of the model is

$$Q = \sum_{\{s_i\}} \sum_{\{t_i\}} e^{-\beta \mathcal{H}}. \tag{2.9}$$

We choose to sum over $\{t_i\}$ first:

$$Q = \sum_{\{s_i\}} e^{-\beta \mathcal{H}_S} Q_C[s_i], \tag{2.10}$$

where

$$Q_C[s_i] = \sum_{\{t_i\}} e^{-\beta \mathcal{H}_C}. \tag{2.11}$$

For the calculation of Q_C, the nonlocal term in $\mathcal{H}_C$ can be made linear in $s_i t_i$ by a Hubbard-Stratonovic transformation [23]:

$$\begin{aligned} Q_C = {} & \left[2\pi\beta q^2 \det v\right]^{-N/2} \\ & \times \int \mathcal{D}\phi \exp\left[-\frac{1}{2}\sum_{jk} \phi_j (\beta q^2 v)^{-1}_{jk} \phi_k\right] \\ & \times \prod_{j=1}^{N} \sum_{t_j = 0,1} \exp\left(i s_j t_j \phi_j + \beta \mu t_j\right). \end{aligned} \tag{2.12}$$

Note that diagonal terms of v_{ij},

$$v_{ii} = \int_{\mathbf{k}} 4\pi / a^3 k^2 \tag{2.13}$$

can be included in Eq.(2.1c) to make the transformation (2.12) well defined. This amounts to a trivial shift of the chemical potential μ since $s_i^2 t_i^2 = t_i$. The sums over $\{t_i\}$ are now done, yielding

$$Q_C = \left[2\pi\beta q^2 \det v\right]^{-N/2} \int \mathcal{D}\phi \exp\left(-S\left[\phi_i, s_i\right]\right), \tag{2.14}$$

where

$$\begin{aligned} S\left[\phi_i, s_i\right] = {} & \frac{1}{2}\sum_{jk} \phi_j (\beta q^2 v)^{-1}_{jk} \phi_k \\ & - \sum_j \ln\left[1 + z \exp(i s_j \phi_j)\right]. \end{aligned} \tag{2.15}$$

The quantity z is the fugacity of charged sites:

$$z = e^{\beta \mu}. \tag{2.16}$$

The partition function has been reduced to a functional integral with an action $S[\phi_i, s_i]$ that consists of a nonlocal Gaussian part and a non-Gaussian local part. It is similar to that of the neutral Coulomb gas. A Gaus-

sian approximation of this nonlinear functional integral is analogous to the Debye-Hückel theory of electrolytes. In the Appendix we show that the Gaussian approximation yields, apart from irrelevant constant terms,

$$\ln Q_C \simeq -\frac{1}{2}\sum_{ij} L_{ij} s_i s_j, \tag{2.17}$$

where L_{ij} is a screened Coulomb potential,

$$\begin{aligned} L_{ij} &= \int_{\mathbf{k}} \hat{L}_k \exp(i\mathbf{k}\cdot\mathbf{r}_{ij}) \\ &\simeq (3fa^4/2\pi\Delta^3 r_{ij}) \exp(-r_{ij}/r_D) \end{aligned} \tag{2.18}$$

with

$$\hat{L}(k) = \frac{fa/\Delta}{1+\Delta^2 k^2/6} \tag{2.19}$$

and

$$r_D = \Delta/\sqrt{6}. \tag{2.20}$$

Combining (2.17) with (2.10) gives

$$Q \propto e^{-\beta\mathcal{F}} = \sum_{\{s_i\}} e^{-\beta\bar{\mathcal{H}}} \tag{2.21}$$

with the reduced spin Hamiltonian

$$\beta\bar{\mathcal{H}} = -\frac{1}{2}\sum_{ij}\beta J_{ij} s_i s_j - \sum_i \beta h_i s_i + \frac{1}{2}\sum_{ij} L_{ij} s_i s_j. \tag{2.22}$$

This Hamiltonian represents a frustrated spin model governed by the competition between a short-range ferromagnetic interaction with length scale a, and a longer-range antiferromagnetic interaction with length scale r_D. The latter is of the order of the surfactant molecule length, 2Δ. We will see that the typical length scale of the mesoscopic domains in bicontinuous microemulsions is determined by the relative strength and range of the two competing interactions.

The Hamiltonian (2.22) can be compared to that of Widom's pioneering and highly influential model [3]. The Hamiltonian of Widom's model is

$$\beta\mathcal{H}_W = -j\sum_{\mathrm{NN}} s_i s_j - 2m\sum_{\mathrm{DN}} s_i s_j - m\sum_{\mathrm{2AN}} s_i s_j, \tag{2.23}$$

where j is the nearest-neighbor (NN) coupling, $2m$ is the coupling between diagonal neighbors (DN), and m couples axial next-nearest-neighbor (2AN) sites. The frustration occurs with $j > 0$ and $m < 0$. The interactions involving m are motivated from the consideration of the bending energy of surfactant layers, but their form is strictly phenomenological. If we neglect L_{ij} for $r_{ij} > 2a$, Eq.(2.22) can be made similar to Eq.(2.23). However, the restrictions with which $\bar{\mathcal{H}}$ becomes $\mathcal{H}_W$ seem arbitrary, without apparent microscopic justification. Unsatisfactory predictions of the Widom model, such as its dependence on lattice symmetry, may be the result of these apparently arbitrary restrictions.

III. MEAN-FIELD THEORY

As a standard approximate treatment of the reduced spin model (2.22), we first use local density mean-field (MF) theory. A reference Hamiltonian is defined in terms of an undetermined field $\{b_i\}$,

$$\mathcal{H}_0 = -\sum_i b_i s_i. \tag{3.1}$$

The reference Hamiltonian is variationally optimized in first-order perturbation theory:

$$\begin{aligned} -\beta\mathcal{F} &\geq -\beta\mathcal{F}_{\mathrm{MF}}[b_i] \\ &= \sum_i \ln(2\cosh\beta b_i) - \beta\langle\bar{\mathcal{H}} - \mathcal{H}_0\rangle_0, \end{aligned} \tag{3.2}$$

where the angular brackets represent

$$\langle\cdots\rangle_0 = \sum_{\{s_i\}}(\cdots)e^{-\beta\mathcal{H}_0} \Big/ \sum_{\{s_i\}} e^{-\beta\mathcal{H}_0}. \tag{3.3}$$

Finding the extremum leads to the familiar self-consistent field equations,

$$m_i = \tanh\left(\beta h_i + \sum_j V_{ij} m_j\right), \tag{3.4}$$

where

$$V_{ij} = \beta J_{ij} - L_{ij}, \tag{3.5}$$

$$m_i = \langle s_i\rangle_0 = \tanh\beta\bar{b}_i, \tag{3.6}$$

and $\{\bar{b}_i\}$ minimizes $\mathcal{F}_{\mathrm{MF}}[b_i]$.

Equivalently, $\mathcal{F}_{\mathrm{MF}}[b_i]$ can be expressed as a functional of m_i. To within a trivial additive constant, this functional is

$$\begin{aligned} \beta F[m_i] = \frac{1}{2}\sum_i \Big[&(1+m_i)\ln(1+m_i) \\ &+(1-m_i)\ln(1-m_i)\Big] \\ &-\sum_i \beta h_i m_i - \frac{1}{2}\sum_{ij} V_{ij} m_i m_j. \end{aligned} \tag{3.7}$$

The minimum of the free-energy functional, $F[\bar{m}_i]$, is at $\bar{m}_i = m_i$, where m_i is given by Eq. (3.4).

With Eq. (2.19) and the Fourier transform of (2.2), Eq. (3.5) gives

$$\hat{V}_k = 2\beta J\sum_x \cos k_x a - \frac{fa/\Delta}{1+\Delta^2 k^2/6}, \tag{3.8}$$

where the sum on x is over the three components of the vector $\mathbf{k}$. Since we are interested in the behavior of the model in the small-k region, we make a small-k expansion of Eq. (3.8):

$$\hat{V}_k \simeq 6\beta J - fa/\Delta + (fa\Delta/6 - \beta J a^2)k^2 - (fa\Delta^3/36)k^4, \tag{3.9}$$

which is valid for $k < \sqrt{6}\Delta^{-1} < a^{-1}$. The lowest-order anisotropic term $(\beta J a^4/12)\sum_x k_x^4$ has been neglected in Eq. (3.9). For the typical values $a \simeq 2$ Å, $\Delta \gtrsim 5$ Å, and $\beta J = \beta\sigma a^2/2 \simeq 0.2$, the neglected term is comparable to $fa\Delta^3 k^4/36$ only for $f < 0.04$. At these small surfactant densities, for $k < 1/a$, the $\mathcal{O}(k^2)$ term dominates over the $\mathcal{O}(k^4)$ term in Eq. (3.9).

The continuum limit of Eq. (3.7) can be derived using Eq. (3.9). It is

$$\beta F[m] = \int \frac{d\mathbf{r}}{a^3}\left[\frac{1}{2}a_2 m^2(\mathbf{r}) + \frac{1}{2}c_1(\nabla m)^2 + \frac{1}{2}c_2(\nabla^2 m)^2 + \frac{1}{12}m^4(\mathbf{r}) - \beta h(\mathbf{r})m(\mathbf{r}) + \mathcal{O}(m^6)\right], \tag{3.10}$$

where

$$a_2 = 1 - 3\beta\sigma a^2 + fa/\Delta\ , \tag{3.11a}$$
$$c_1 = \beta\sigma a^4/2 - fa\Delta/6\ , \tag{3.11b}$$
$$c_2 = fa\Delta^3/36. \tag{3.11c}$$

The correlation function $S_{ij} = \langle s_i s_j\rangle = S(r_{ij})$ can be computed from Eq. (3.10) through the identity

$$S^{-1}(|\mathbf{r} - \mathbf{r}'|) = \left.\frac{\delta^2\beta F}{\delta m(\mathbf{r})\delta m(\mathbf{r}')}\right|_{h(\mathbf{r})=m(\mathbf{r})=0}, \tag{3.12}$$

where $S^{-1}(|\mathbf{r} - \mathbf{r}'|)$ denotes the functional inverse of the correlation function. Evaluation yields

$$\hat{S}_k = \frac{1}{1 - \hat{V}_k} \tag{3.13}$$

or with Eq.(3.9),

$$\hat{S}_k \simeq \frac{1}{a_2 + c_1 k^2 + c_2 k^4}. \tag{3.14}$$

Teubner and Strey [12] first suggested the form (3.14) for the structure factor of microemulsions. The form is motivated from a Landau-Ginzburg expansion of the free-energy functional. In this construction, a_2, c_1, and c_2 are arbitrary phenomenological parameters. With these three fitting parameters, various scattering data of microemulsions can be accurately fit for k up to the microscopic cutoff k_c. Equations (3.11) connect our microscopic model parameters to the phenomenological parameters of this theory.

The mean-field phase diagram is obtained by global minimization of Eq. (3.10). Restricting ourselves to the case of oil-water symmetry, $h(\mathbf{r}) = 0$, continuous phase transitions occur between the paramagnetic (mixed) phase and modulated phases when the coefficient of the quadratic $|\hat{m}_\mathbf{k}|^2$ changes sign at some wave vector, k_m. The case of $k_m = 0$ corresponds to oil-water phase separation. For $c_1 > 0$, the mean-field expression predicts a transition line at $a_2 = 0$ or $2/\beta\sigma a^2 \equiv T^* = 6/(1 + fa/\Delta)$. Here, $k_m = 0$. This line is graphed as the solid curve in Fig. 1. It is the line of oil-water demixing criticality as a function of surfactant volume fraction, f. This critical line terminates at the point where $c_1 = 0$. It is continued for $c_1 < 0$ by $c_1 = -2(a_2 c_2)^{1/2}$, depicted by the dashed line in Fig. 1. Here, $k_m = (-c_1/2c_2)^{1/2}$. The singularity in the mean-field structure factor at these finite wave vectors suggests the onset of modulated long-range order as in a lamellar phase. In actuality, this line represents a limit of stability of mean-field theory. A correct analysis of the phase diagram for temperatures below the solid and dashed lines of Fig. 1 must account for nonlinear contributions to the free energy. These considerations will delineate regions of coexistence and predict that the transition to a lamellar phase is first order.

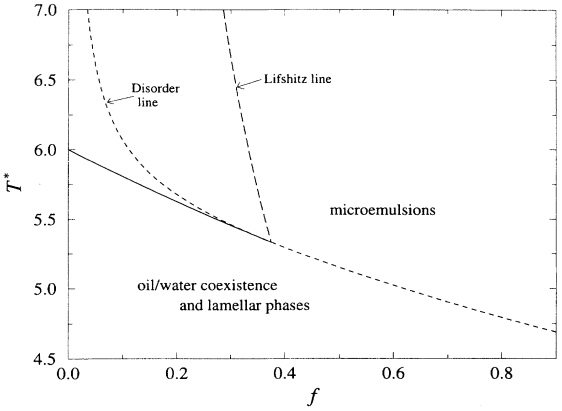

FIG. 1. Mean-field phase boundaries surrounding the microemulsion phase: reduced temperature $T^* = 2/\beta\sigma a^2$ vs the volume fraction of surfactant f at constant $\Delta = 6$ Å and $a = 2$ Å. The solid line separates the homogeneous mixture and oil-water phase separated region. The water-water correlation function of the homogeneous phase oscillates to the right of the disorder line. This line continues smoothly to the stability line separating microemulsions from modulated lamellar phases. The long-dashed line, marking the onset of bicontinuity, is the Lifshitz line.

The treatment of coexistence is beyond the scope of the current analysis. In particular, the Debye-Hückel approach used in obtaining the reduced Hamiltonian (2.22) is derived with the assumption that the system is macroscopically homogeneous. Given the similarity between the reduced Hamiltonian and Widom's (2.23), one thus understands why Widom's model predicts a continuous transition to oil-water coexistence. First-order transitions are observed experimentally. The derivation of the reduced Hamiltonian (2.22) can be generalized to remove the limitation of homogeneity, as we show in forthcoming work [24]. For the current paper, we confine our attention to the regime above the solid and dashed lines of Fig. 1. In this regime, what is most significant is what mean-field theory predicts about the stability of microemulsions.

Note that in the absence of surfactant, i.e., $f = 0$, we have $c_1 > 0$ and $c_2 = 0$. As such, with $f = 0$, Eq. (3.14) has the usual Ornstein-Zernike form. Increasing surfactant density brings the system to the disorder line where

$c_1 = 2(a_2c_2)^{1/2}$. Beyond this line, the real-space correlation function oscillates [12]. At yet higher surfactant densities, the system reaches the Lifshitz line, where $c_1 = 0$ or $f = 6a/T^*\Delta \equiv f_L$. At any higher density, the structure factor peaks at a nonzero wave vector, characteristic of microemulsions with microphase separation.

The amplitude of these finite-wave-vector correlations is governed in the mean-field theory by the size of a_2 and therefore the proximity to criticality. Fluctuations considerably lower the line of critical temperatures from the predictions of mean-field theory, as previously shown in studies of other lattice models [2,25–27]. Therefore, an improvement to the mean-field theory result is necessary for quantitative comparison with experiment. We consider now an improvement that allows for fluctuations.

IV. ROLE OF FLUCTUATIONS

To include part of the effect of fluctuations, we go back to the reduced spin Hamiltonian (2.22) and use a Hubbard-Stratonovic transformation to express the partition function as a functional integral [23]. In particular,

$$Q \propto \int \mathcal{D}\psi \exp\left(-A[\psi_i]\right), \tag{4.1}$$

where

$$A[\psi_i] = \frac{1}{2}\sum_{ij}(\psi_i - \beta h_i)\hat{V}_{ij}^{-1}(\psi_j - \beta h_j) - \sum_i \ln\cosh\psi_i. \tag{4.2}$$

The spin-spin correlation function S_{ij} is related to the correlation of the field

$$g_{ij} = \frac{\int \mathcal{D}\psi(\psi_i\psi_j)\exp\left(-A[\psi_i]\right)}{\int \mathcal{D}\psi \exp\left(-A[\psi_i]\right)} \tag{4.3}$$

by

$$S_{ij} = \frac{\partial^2 \ln Q}{\partial\beta h_i \partial\beta h_j}\bigg|_{h=0} = -V_{ij}^{-1} + \sum_{kl} V_{ik}^{-1} g_{kl} V_{lj}^{-1}, \tag{4.4}$$

or in k space,

$$\hat{S}_k = -\hat{V}_k^{-1} + \hat{V}_k^{-2}\hat{g}_k. \tag{4.5}$$

The last term in the functional (4.2) can be expanded in powers of ψ_i. A Gaussian approximation to Eq. (4.3) is obtained by neglecting all terms in the expansion beyond quadratic order. This approximation gives $\hat{g}_k = 1/(\hat{V}_k^{-1} - 1)$ whereupon, through Eq. (4.5), we get the mean-field result (3.13). To account approximately for higher-order terms, we estimate their effects with an additional quadratic term, its coefficient λ to be determined self-consistently:

$$A[\psi_i, h = 0] \simeq \frac{1}{2}\sum_{ij}\psi_i V_{ij}^{-1}\psi_j + \frac{1}{2}\sum_i(\lambda - 1)\psi_i^2. \tag{4.6}$$

Now $\hat{g}_k^{-1} \simeq \hat{V}_k^{-1} - (1 - \lambda)$, and from Eq. (4.5),

$$\hat{S}_k = \frac{1}{(1-\lambda)^{-1} - \hat{V}_k}. \tag{4.7}$$

The k-independent part of $\hat{S}_k$ is renormalized by the inclusion of λ. To determine λ or equivalently

$$\bar{a}_2 = a_2 + \lambda/(1-\lambda), \tag{4.8}$$

we impose the hard spin condition $(1/N)\sum_{\mathbf{k}}\hat{S}_k = S_{ii} = \langle s_i^2\rangle = 1$ [28]:

$$1 = \int_{\mathbf{k}}\left[(1-\lambda)^{-1} - \hat{V}_k\right]^{-1}. \tag{4.9}$$

With Eq. (3.9), the integral can be done approximately by taking $k_c \to \infty$. The approximation is justified in the mesoscopic regime, $k < 1/\Delta$. The result is

$$\hat{S}_k = \frac{1}{\bar{a}_2 + c_1k^2 + c_2k^4}, \tag{4.10}$$

where

$$\bar{a}_2 = \frac{c_2}{4}\left(\frac{a^6}{16\pi^2 c_2^2} - \frac{c_1}{c_2}\right)^2. \tag{4.11}$$

The constants c_1 and c_2 are given by Eqs. (3.11b) and (3.11c). Fourier inversion of Eq. (4.10) gives the real-space correlation

$$S_{ij} = \frac{\sin(\kappa r_{ij})}{\kappa r_{ij}}\exp\left(-r_{ij}/\xi\right), \tag{4.12}$$

where

$$\kappa = \left[\frac{1}{2}\left(\frac{\bar{a}_2}{c_2}\right)^{1/2} - \frac{c_1}{4c_2}\right]^{1/2} \tag{4.13}$$

and

$$\xi = \left[\frac{1}{2}\left(\frac{\bar{a}_2}{c_2}\right)^{1/2} + \frac{c_1}{4c_2}\right]^{-1/2}. \tag{4.14}$$

The augmentation of the Gaussian approximation to enforce the hard spin condition, Eqs. (4.7) and (4.9), is a mean spherical or optimized random-phase approximation [29–31]. The development given here follows those of Mühlschlegel and Zittartz [32]. It provides the foundation for the random wave model of bicontinuous phases [16–19]. In the random wave model, Cahn's model of spinodal decomposition [33] is adapted to the description of bicontinuous phases by constructing the density field $\rho(\mathbf{r})$ from a random Gaussian field $\psi(\mathbf{r})$ through a transformation

$$\rho(\mathbf{r}) = c(\psi(\mathbf{r})). \tag{4.15}$$

The average and spectral density of the Gaussian variable $\psi(\mathbf{r})$ determines the statistical properties of the density field $\rho(\mathbf{r})$ by Eq. (4.15). Teubner [17] used a step function for this transformation. In our case, the spin that coincides with the density is related to the renormal-

ized Gaussian field ψ_i by an invertible transformation. Namely,

$$s_i = \tanh \psi_i \ , \tag{4.16}$$

as can be verified from Eq. (4.2) by replacing $\psi_i \rightarrow \psi_i + \beta h_i$ and differentiating to obtain $\langle s_i \rangle = \partial \ln Q / \partial \beta h_i$. Deem and Chandler [10] used the transformation (4.16) in the density functional version of the model (2.1) to analyze the interfacial structure of bicontinuous phases. For bicontinuous phases with large microphase separated domains, the transformation function differs from its asymptotic values for only a small fraction of the total system. For this situation, the distinction between a continuous transformation and a step function transformation is probably irrelevant. To the extent the distinction is irrelevant, the theory presented here provides a derivation of the random wave model of bicontinuous microemulsions.

V. COMPARISON WITH EXPERIMENT

For comparison with experimental SANS data, we assume the density of water is given by $\rho_0(s_i + 1)/2$ where ρ_0 is the bulk density of water. This correspondence entails a small error, as $s_i = 1$ does not by itself distinguish polar solvent from polar surfactant segment. To the extent this error is negligible, the scattering cross section difference between water and oil, $I(k)$, is proportional to the spin-spin structure factor, Eq.(4.10). Thus,

$$I(k) = \frac{a^3(\Delta n)^2/4}{\bar{a}_2 + c_1 k^2 + c_2 k^4}, \tag{5.1}$$

where Δn is the difference of the scattering length densities between water and oil. This formula is valid for k small compared to $2\pi/\Delta$. At larger wave vectors, or for film scattering, the general analysis of the preceding section, leading to the random wave model, is still accurate. In this section, however, we confine our attention to bulk scattering in the small wave-vector regime and test our predictions of the coefficients in the Teubner-Strey structure factor, (5.1).

The maximum of $I(k)$ occurs at $k = k_m$ given by

$$k_m = (\sqrt{3}/\Delta)(1 - 3\beta\sigma a^3/f\Delta)^{1/2} \tag{5.2}$$

for $f > f_L = 3\beta\sigma a^3/\Delta$. At volume fractions, f, less than that of the Lifshitz line, f_L, $k_m = 0$. The length $D = 2\pi/k_m$ is a measure of the domain size in the microphase separated structure. An alternative measure used by Strey and co-workers [12–14] is $d = 2\pi/\kappa$ given by Eq. (4.13). The alternative is less general than $2\pi/k_m$ in the sense that it is restricted to the form of the correlation (4.12) and therefore to the Teubner-Strey form (4.10) or (5.1). With increasing f, D monotonically decreases from $D = \infty$ at $f = f_L$, asymptotically approaching $D \rightarrow 2\pi\Delta/\sqrt{3}$, roughly the length scale of surfactant molecules. Figure 2 shows a plot of k_m as a function of f and compared with experiment [14]. The parameters

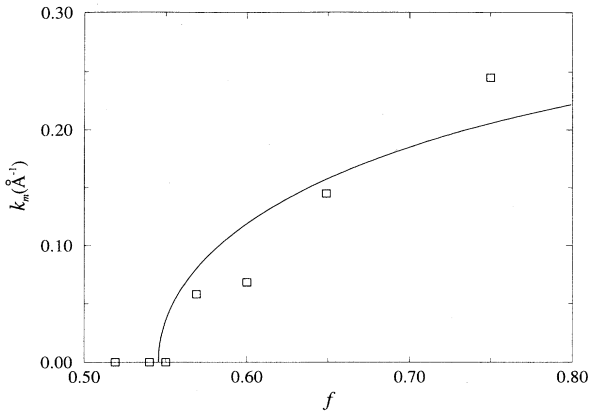

FIG. 2. The position of the peak maximum given by Eq. (5.2) as a function of surfactant volume fraction, f, at constant $\Delta = 4.4$ Å, $\beta\sigma = 0.1$ Å^{-2}, and $a = 2$ Å. The Lifshitz line is at $f = 0.545$. The rectangles are the data points for water-octane–C_4E_1 samples from Ref. [14] (three points of which are shown in Table I).

used for the plot ($\Delta = 4.4$ Å, $\beta\sigma = 0.1$ Å^{-2}, and $a = 2$ Å) are in accord with the estimates discussed in Sec. II.

Similar behavior has been observed in many SANS experiments on three-component microemulsion systems. Strey and co-workers [13,14] have fit bulk-contrast SANS spectra of water-octane-C_iE_j microemulsion systems into the Teubner-Strey form [C_iE_j is an abbreviation for CH_3-$(CH_2)_{i-1}$-$(OCH_2CH_2)_j$-OH]. In Table I, with the fitting parameter values in Ref. [14], we have taken $a = 2$ Å and determined Δn, σ, and Δ using Eqs. (3.11b), (3.11c), (4.11), and (5.1) [34]. Each sample consists of D_2O-C_8H_{18}-C_4E_1 with equal volume fractions of water and oil. The expected theoretical value of Δn is $\Delta n = 6.98 \times 10^{10}$ cm^{-2} [13]. The values of σ compare favorably to the typical values of oil-water surface tension $\sigma \simeq 0.1 k_B T$ Å^{-2} (for water–n-octane, $\sigma = 0.126 k_B T$ Å^{-2} at $T = 20\,^{\circ}$C [20]). The values of surfactant length scale Δ are also reasonable since 2Δ is expected to be approximately the length of the surfactant molecule. However, the very small values of Δ, C_4E_1 being one of the smallest surfactants available, bring k_m near the microscopic region. We expect our theory to be more reliable for systems with larger surfactant molecules.

Table II with Figs. 3 and 4 show the result of fitting the SANS spectra of D_2O–n-octane–$C_{12}E_5$ systems from

TABLE I. Parameters determined by comparing Eq. (5.1) with the fit parameters from Ref. [13]. Each sample consists of D_2O–C_8H_{18}–C_4E_1. Volume fractions were calculated from the concentrations γ in weight fractions using known densities of three components assuming ideal mixing. $a = 2$ Å in all cases.

γ (wt %)	f	Δn (10^{10} cm^{-2})	σ ($k_B T$ Å^{-2})	Δ (Å)
52	0.519	5.00	0.106	4.35
57	0.569	4.18	0.101	4.35
65	0.649	3.78	0.098	4.12

TABLE II. Parameters determined by fitting Eq. (5.1) to SANS spectra of D_2O–n-octane–$C_{12}E_5$ from Ref. [1]: Samples 1–3; and D_2O–n-decane–AOT from Ref. [15]: Samples 4–6. Volume fractions f were calculated from the weight fractions γ reported in Ref. [1]. $a = 2$ Å in all cases. Figures 3 and 4 show the spectra.

Sample	f	Δn (10^{10} cm^{-2})	σ (k_BT Å^{-2})	Δ (Å)
1	0.0566	7.99	0.0656	28.3
2	0.121	7.98	0.0954	19.5
3	0.200	8.24	0.113	14.9
4	0.181	6.41	0.0920	13.0
5	0.237	5.96	0.103	11.5
6	0.323	5.79	0.111	9.78

Ref. [1] and D_2O–n-decane–AOT systems from Ref. [15] (AOT is an abbreviation for sodium bis-2-ethyl hexyl sulphosuccinate). Again, Δ correlates reasonably with the approximate size of the surfactant molecule in the samples. For a given set of oil and surfactant species, the systematic variations of σ and Δ seem to indicate an inadequacy of the minimalist model Hamiltonian (2.1). Most likely, it is the result of assuming the same value for J_{ij} irrespective of whether i and j refer to either solvent (oil or water) or solute (surfactant head or tail). Nevertheless, this theory, based upon well-defined intrinsic length scales of the order of angstroms, is remarkably successful in predicting the microscopic correlations on mesoscopic scales.

Figure 3 is graphed as a log-log plot to exhibit the onset of Porod's k^{-4} scaling [35]. This behavior is a characteristic of a bicontinuous systems with narrow interfaces. For the case with largest domains, graph (a), Porod's scaling holds over an order of magnitude in k.

The large scattering cross section at $k = 0$ indicates a small value of $\bar{a}_2$. Values of $\bar{a}_2$ for the structure factors graphed in Figs. 4 and 3 range from 10^{-3} to 10^{-7}.

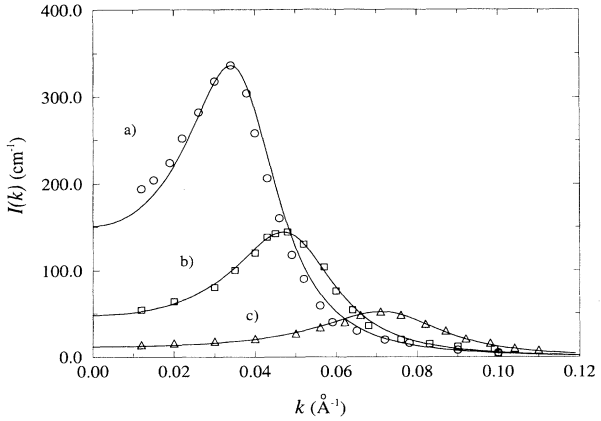

FIG. 3. SANS spectra of D_2O–n-decane–AOT systems at varying surfactant volume fraction, f. Data are from Ref. [15]; (a) $f = 0.181$, (b) $f = 0.237$, and (c) $f = 0.323$. The corresponding solid lines are the result of fitting with Eq. (5.1). Table II shows the corresponding parameter values.

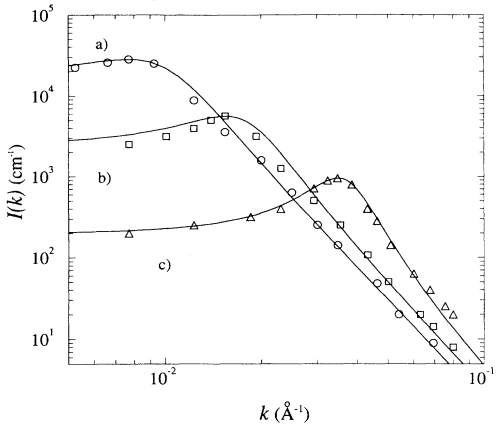

FIG. 4. SANS spectra of D_2O–n-octane–$C_{12}E_5$ systems at varying surfactant volume fraction, f. Data are from Ref. [1]; (a) $f = 0.0566$, (b) $f = 0.121$, and (c) $f = 0.200$. The corresponding solid lines are the result of fitting with Eq. (5.1). See Table II for the parameter values.

At the same time, λ is either positive or negative, with magnitude typically near 0.1. Renormalization of a_2 is therefore significant, causing $a_2 \simeq -\lambda$. See Eq. (4.8). Unrenormalized mean-field theory, Eq. (3.14), could be used to fit large structure factors. But the bare a_2 would then be very small. Mean-field theory would thus associate bicontinuity with near criticality of oil-water demixing. In the renormalized theory, and in nature, large structure factors can occur relatively far from the oil-water demixing critical line.

Recently there have been experimental suggestions of qualitative differences in the domain structures between short-chain and long-chain surfactant systems [13,36]. Our result (5.2) allows us to examine the behavior of the mesoscopic domain as we increase the chain length of surfactant while keeping the volume fraction constant. The relative amphiphilicity of the surfactant increases as we increase the chain length. k_m grows from zero as Δ increases from its value at the Lifshitz line, $\Delta_L = 3\beta\sigma a^3/f$. This trend reverses, however, for $\Delta > \Delta_C = 9\beta\sigma a^3/2f$. See Fig. 5.

Table III shows the result of fitting the SANS spectra of C_4E_1, C_6E_2, and C_8E_3 systems [13]. Δ systematically increases by ~ 4 Å as we successively add —CH_2-CH_2-O-CH_2-CH_2— bonds into the surfactant molecule. Since the three samples are at different densities, it is not clear

TABLE III. Parameter values determined by comparing Eq. (5.1) with the fit parameters from Ref. [13]. The solutions are water and n-C_8D_{18} with added C_4E_1 (sample 1), C_6E_2 (sample 2), and C_8E_3 (sample 3). $a = 2$ Å in all cases.

Sample	f	Δn (10^{10} cm^{-2})	σ (k_BT Å^{-2})	Δ (Å)	k_m (Å^{-1})
1	0.520	5.22	0.106	4.23	0
2	0.333	5.80	0.106	8.12	0.0537
3	0.212	6.38	0.104	12.7	0.0360

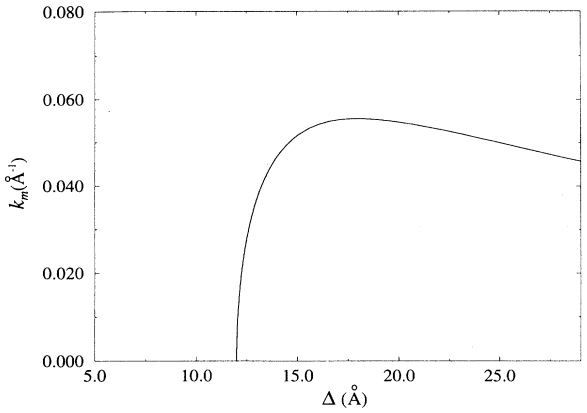

FIG. 5. The position of the structure factor peak maximum, k_m, given by Eq. (5.2) with increasing surfactant chain length, Δ, at $f = 0.2$, $a = 2$ Å, and $\beta\sigma = 0.1$ Å^{-2}. k_m jumps up from zero at the Lifshitz line and increases with increasing Δ for $\Delta_L < \Delta < \Delta_C$, and decreases for $\Delta > \Delta_C$. $\Delta_L = 12$ Å and $\Delta_C = 18$ Å in this case.

whether the nonmonotonic behavior of k_m down the column of Table III is due to the increasing chain length. Figure 6 shows a three-dimensional plot of k_m as a function of density and chain length with the typical values of σ and a: $\sigma = 0.1 k_B T$ Å^{-2} and $a = 2$ Å. Shown together are cubic boxes centered at the data points (Δ, f, k_m) with k_m calculated by Eq. (5.2) for each of the fit parameters in Tables I–III. All of the data points seem to be restricted to the short-chain regime $\Delta < \Delta_C$. Experimental attempts to verify the $\Delta > \Delta_C$ regime will be worthwhile.

VI. DISCUSSION

The central result of this paper is the analytical expression for the long-wavelength structure factor, Eq. (4.10).

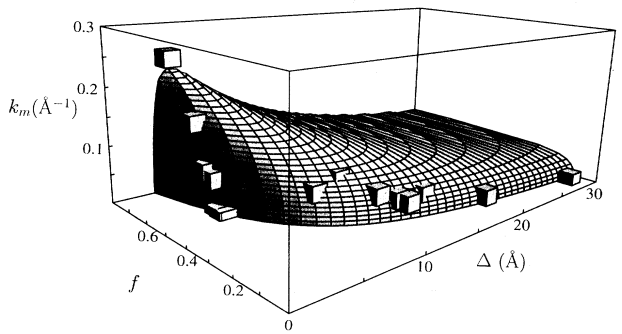

FIG. 6. Three-dimensional plot of the position of peak maximum k_m as a function of volume fraction f and chain length Δ from Eq. (5.2) with $\sigma = 0.1$ Å^{-2} and $a = 2$ Å. The cubic boxes represent the result of fitting experimental data points from [1,12–15], some of which are shown in Tables I–III. The centers of the boxes correspond to the points (Δ, f, k_m) with k_m calculated by Eq. (5.2).

Its dependence upon k is standard. But the remarkably simple yet nontrivial connections between its coefficients $\bar{a}_2$, c_1, and c_2 and physical parameters such as surfactant chain length and density are new. The comparisons we have made with existing experimental data on scattering from microemulsions support the theory we have derived. Further experimentation seems necessary, however, to fully test the predictions of the theory.

One issue not addressed in this paper concerns the nature of the surfactant interfaces that divide oil-rich and water-rich domains in the microemulsions. In view of Fig. 6, we see that some microemulsions can have relatively small domains. Surfactant monolayers in these cases are relatively easy to bend. The standard interface model [37] may not work well for those systems since the boundaries between oil and water will be murky and diffuse. Deem and Chandler analyzed this behavior showing that microemulsions with long correlation lengths can exist without relatively narrow interfaces [10]. A more complete description of this behavior and its relationship to bending moduli are worthy of future investigation.

Modulated phases and phase coexistence also merit treatment within the context of the charge frustrated Ising model. Analytical expressions for phase boundaries will provide thermodynamically testable predictions of the model. It remains to be seen what experimental phenomena require extension beyond its most elementary form involving only one fundamental energy and two microscopic lengths.

ACKNOWLEDGMENTS

We thank S.-H. Chen and S. Singer for their helpful suggestions on this work. This research has been supported by the National Science Foundation and the Office of Naval Research.

APPENDIX

In this appendix, we show that a Gaussian approximation to the functional integral (2.14) yields the reduced spin-1/2 lattice model (2.22).

Expanding Eq.(2.15) through quadratic order in ϕ_i gives the Gaussian action

$$S_G[\phi_i, s_i] = -Nz + \frac{1}{2}\sum_{jk}\phi_i(\beta q^2 v)^{-1}_{jk}\phi_k + \frac{z}{2}\sum_j \phi_j^2 - iz\sum_j s_j\phi_j \qquad \text{(A1)}$$

for small z. With this action, the functional integration in Eq. (2.14) gives

$$Q_C = C\exp\left(-\frac{1}{2}\sum_{ij}L_{ij}s_i s_j\right), \qquad \text{(A2)}$$

where

$$C = \left(\frac{e^{2z} \det L}{z^2 \beta q^2 \det v} \right)^{N/2}. \quad \text{(A3)}$$

The Gaussian kernel L_{ij} is given in k space by

$$\hat{L}_k = \frac{z}{1 + \bar{\rho}\Delta^2 k^2/6z}. \quad \text{(A4)}$$

The condition of self-consistency for the reduced density of surfactant, $\bar{\rho} = \rho a^3$, is

$$2\bar{\rho} = \frac{1}{N} \frac{\partial \ln Q}{\partial \ln z}. \quad \text{(A5)}$$

The factor of 2 accounts for the fact that there are two charged sites per surfactant molecule.

The full partition function Q, Eq. (2.10), must be obtained for the evaluation of the right-hand side of Eq. (A5). However, to a good approximation, only the term $\ln C$ from Eq. (A2) needs to be considered in the absence of broken symmetry. The demonstration is as follows. From Eqs. (2.10) and (A2),

$$\ln Q(z) = \ln C(z) + \ln \sum_{\{s_i\}} \exp\left(-\beta \mathcal{H}_S - \frac{1}{2} \sum_{ij} L_{ij}(z) s_i s_j \right). \quad \text{(A6)}$$

To estimate the second term in Eq. (A6), we use the mean-field theory. The same method illustrated in Sec. III yields for $h_i = 0$,

$$\ln [Q(z)/C(z)] = (6\beta J - zu1)m^2 - m^4/12 + O(m^6). \quad \text{(A7)}$$

In Eq. (A7), $m = \langle s_i \rangle$. This quantity is zero in the absence of broken symmetry. Therefore, $\ln(Q/C)$ is very small. Hence, Eq. (A5) is approximately

$$2\bar{\rho} \simeq \frac{1}{N} \frac{\partial \ln C}{\partial \ln z}. \quad \text{(A8)}$$

With Eq. (A3), this approximation gives

$$2x = 1 - \frac{1}{2} \int_{\mathbf{k}} \frac{1}{1 + x\Delta^2 k^2/6}, \quad \text{(A9)}$$

where $x = \bar{\rho}/z$. The integral in Eq. (A9) depends on the cutoff k_c. The following manipulations, however, allow the extraction of the cutoff-independent part. The remainder can be fixed by the normalization condition (2.4):

$$\int_{\mathbf{k}} \frac{1}{1 + x\Delta^2 k^2/6} = \frac{a^3}{2\pi^2} \int_0^{k_c} \frac{k^2 dk}{1 + x\Delta^2 k^2/6} = \frac{3a^3}{\pi^2 x \Delta^2} \left(k_c - \int_0^{k_c} \frac{dk}{1 + x\Delta^2 k^2/6} \right). \quad \text{(A10)}$$

Using Eq. (2.5) for the first term and taking $k_c \simeq \infty$ for the integral in Eq. (A10), Eq. (A9) becomes

$$2x = 1 - \frac{(6/\pi)^{4/3}}{4x} \left(\frac{a}{\Delta} \right)^2 + \frac{3(3/2)^{1/2}}{2\pi x^{3/2}} \left(\frac{a}{\Delta} \right)^3. \quad \text{(A11)}$$

As Δ/a increases, the solution to Eq. (A11) rapidly converges to $x \simeq 1/2$. Therefore, we get

$$2\bar{\rho} \simeq z. \quad \text{(A12)}$$

This result agrees with the low-density limit of the fugacity series in the general grand canonical system. Combining Eqs. (2.8), (A2), (A4), and (A12) yields Eq. (2.17) with Eq. (2.19).

Nontrivial coupling between the two densities, m and ρ, must be considered in the cases of phase coexistence (i.e., states of broken symmetry). The reduced spin Hamiltonian (2.22) and the mean-field treatment described in Sec. III must be generalized to cover such cases [24].

[1] A summary of various experimental techniques is provided by M. Kahlweit, R. Strey, D. Hasse, H. Kunieda, T. Schmeling, B. Faulhaber, L. Magid, O. Söderman, P. Stilbs, J. Winkler, A. Dittrich, and W. Jahn, J. Colloid Interface Sci. **118**, 436 (1987).

[2] G. Gompper and M. Schick, *Self-Assembling Amphiphilic Systems* (Academic, San Diego, 1994).

[3] B. Widom, J. Chem. Phys. **84**, 6943 (1986).

[4] K. A. Dawson, M. D. Lipkin, and B. Widom, J. Chem. Phys. **88**, 5149 (1988).

[5] F. H. Stillinger, J. Chem. Phys. **78**, 4654 (1983).

[6] L. Leibler, Macromolecules **13**, 1602 (1980); T. Ohta and K. Kawasaki, *ibid.* **19**, 2621 (1986).

[7] D. Chandler, J. Chem. Phys. **67**, 1113 (1977).

[8] M. M. Hurley and S. J. Singer, J. Phys. Chem. **96**, 1938 (1992); **96**, 1951 (1992).

[9] M. W. Deem and D. Chandler, Phys. Rev. E **49**, 4268 (1994).

[10] M. W. Deem and D. Chandler, Phys. Rev. E **49**, 4276 (1994).

[11] D. Wu, D. Chandler, and B. Smit, J. Phys. Chem. **96**, 4077 (1992).

[12] M. Teubner and R. Strey, J. Chem. Phys. **87**, 3195 (1987).

[13] K.-V. Schubert and R. Strey, J. Chem. Phys. **95**, 8532 (1991).

[14] K.-V. Schubert, R. Strey, S. R. Kline, and E. W. Kaler, J. Chem. Phys. **101**, 5343 (1994).

[15] M. Kotlarchyk, S.-H. Chen, J. S. Huang, and M. W. Kim, Phys. Rev. Lett. **53**, 941 (1984).

[16] N. F. Berk, Phys. Rev. Lett. **58**, 2718 (1987).

[17] M. Teubner, Europhys. Lett. **14**, 403 (1991).

[18] S. Marčelja, J. Phys. Chem. **94**, 7259 (1990); P. Pieruschka and S. Marčelja, J. Phys. (France) II **2**, 235 (1992); P. Pieruschka and S. A. Safran, J. Phys. Condens. Matter **6**, A357 (1994).

[19] S. H. Chen, S. L. Chang, R. Strey, J. Samseth, and K. Mortensen, J. Phys. Chem. **95**, 7427 (1991).
[20] R. C. Weast, *CRC Handbook of Chemistry and Physics*, 68th ed. (CRC Press, Boca Raton, FL, 1987), p. F-34.
[21] Stillinger's formula [5] is

$$\Delta^2 = \Delta^2_{P_S H_S}/n_{P_S} n_{H_S} - \Delta^2_{P_S P_S}/2n^2_{P_S} - \Delta^2_{H_S H_S}/2n^2_{H_S},$$

where n_{P_S} and n_{H_S} are the numbers of polar and hydrophobic segments, respectively in a surfactant, and $\Delta^2_{\alpha\gamma}$ is the mean-square distance between α and γ groups (α, $\gamma = P_S$ or H_S) in a surfactant molecule.
[22] P. J. Flory, *Principles of Polymer Chemistry* (Cornell Univ. Press, Ithaca, 1953).
[23] See, for example, G. Parisi, *Statistical Field Theory* (Addison-Wesley, Redwood City, CA, 1988), pp. 209–213.
[24] H.-J. Woo, C. Carraro, and D. Chandler (to be published).
[25] G. Gompper and M. Schick, Phys. Rev. A **42**, 2137 (1990); A. Hansen, M. Schick, and D. Stauffer, *ibid.* **44**, 3686 (1991).
[26] Y. Levin and K. A. Dawson, Phys. Rev. A **42**, 1976 (1990); Y. Levin, C. J. Mundy, and K. A. Dawson, *ibid.* **45**, 7309 (1992).
[27] M. W. Matsen and D. E. Sullivan, Phys. Rev. E **51**, 548 (1995).
[28] In the usual Hartree approximation to this field theory, it is assumed that $\lambda = \langle \phi_i^2 \rangle /2$, which leads to the self-consistent equation

$$2\lambda = \int_{\mathbf{k}} \hat{g}_k = \int_{\mathbf{k}} \left[\hat{V}_k^{-1} - (1-\lambda)\right]^{-1}$$
$$= \left\{1 - \int_{\mathbf{k}} \left[1 - (1-\lambda)\hat{V}_k\right]^{-1}\right\} \Big/ (\lambda - 1).$$

But from Eq. (4.5), this relationship is equivalent to

$$(1-\lambda)(1 + 2\lambda - 2\lambda^2) = \int_{\mathbf{k}} \hat{S}_k.$$

The Hartree approximation is therefore generally inconsistent with the hard spin condition $\int_{\mathbf{k}} \hat{S}_k = 1$.
[29] J. L. Lebowitz and J. K. Percus, Phys. Rev. **144**, 251 (1966).
[30] J. K. Percus and G. J. Yevick, Phys. Rev. **136**, B290 (1966).
[31] H. C. Anderson and D. Chandler, J. Chem. Phys. **55**, 1497 (1971).
[32] B. Mühlschlegel and H. Zittartz, Z. Phys. **175**, 553 (1963); R. Micnas, Physica (Amsterdam) **98A**, 403 (1979).
[33] J. W. Cahn, J. Chem. Phys. **42**, 93 (1965).
[34] Note that our definition of a_2, c_1, and c_2 differs from the one in Refs. [12–14] by the normalization factor $a^3(\Delta n)^2/4$.
[35] G. Porod, Kolloid Z. **124**, 83 (1951); **125**, 51 (1952).
[36] M. Kahlweit, R. Strey, and G. Busse, Phys. Rev. E **47**, 4197 (1993).
[37] W. Helfrich, Z. Naturforsch. **28c**, 693 (1973).

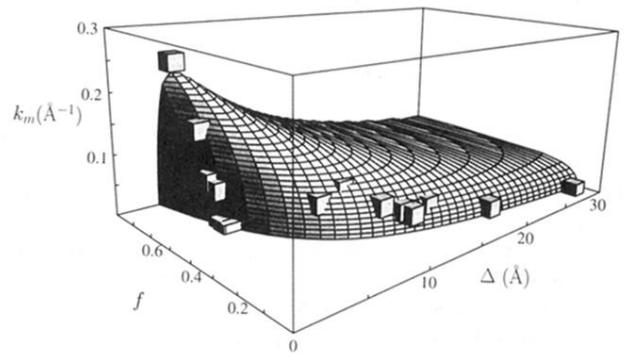

FIG. 6. Three-dimensional plot of the position of peak maximum k_m as a function of volume fraction f and chain length Δ from Eq. (5.2) with $\sigma = 0.1$ Å^{-2} and $a = 2$ Å. The cubic boxes represent the result of fitting experimental data points from [1,12–15], some of which are shown in Tables I–III. The centers of the boxes correspond to the points (Δ, f, k_m) with k_m calculated by Eq. (5.2).